Improving MFI-UF constant flux to more accurately predict particulate fouling in RO systems

Quantifying the effect of membrane surface porosity

Abunada, Mohanad; Dhakal, Nirajan; Andyar, William Z.; Ajok, Pamela; Smit, Herman; Ghaffour, Noreddine; Schippers, Jan C.; Kennedy, Maria D.

DOI
10.1016/j.memsci.2022.120854

Publication date
2022

Document Version
Final published version

Published in
Journal of Membrane Science

Citation (APA)
Abunada, M., Dhakal, N., Andyar, W. Z., Ajok, P., Smit, H., Ghaffour, N., Schippers, J. C., & Kennedy, M. D. (2022). Improving MFI-UF constant flux to more accurately predict particulate fouling in RO systems: Quantifying the effect of membrane surface porosity. *Journal of Membrane Science*, *660*, Article 120854. https://doi.org/10.1016/j.memsci.2022.120854

Journal of Membrane Science 660 (2022) 120854

Contents lists available at ScienceDirect

Journal of Membrane Science

journal homepage: www.elsevier.com/locate/memsci

Improving MFI-UF constant flux to more accurately predict particulate fouling in RO systems: Quantifying the effect of membrane surface porosity

Mohanad Abunada [a,b,*], Nirajan Dhakal [a], William Z. Andyar [a], Pamela Ajok [a], Herman Smit [c], Noreddine Ghaffour [d], Jan C. Schippers [a], Maria D. Kennedy [a,b]

[a] IHE-Delft Institute for Water Education, Water Supply, Sanitation and Environmental Engineering Department, Westvest 7, 2611 AX, Delft, the Netherlands
[b] Delft University of Technology, Faculty of Civil Engineering, Stevinweg 1, 2628 CN Delft, the Netherlands
[c] PWN, Rijksweg 501, 1991 AS Velserbroek, the Netherlands
[d] King Abdullah University of Science and Technology (KAUST), Thuwal, 23955-6900, Saudi Arabia

ARTICLE INFO

Keywords:
MFI-UF
Particulate fouling
Cake filtration
Membrane surface porosity
Washed polystyrene particles

ABSTRACT

This study aimed to quantify the effect of membrane surface porosity on particulate fouling predicted by the MFI-UF method at constant flux. Firstly, the surface porosity of polyethersulfone UF membranes (5–100 kDa) was determined using ultra-high resolution SEM. Thereafter, the MFI-UF was measured using suspensions of polystyrene particles (75 nm), which were pre-washed to remove surfactant and particle fractions smaller than the pores of MFI-UF membranes, thus ensuring complete retention of particles during MFI-UF measurements. Consequently, the MFI-UF values of washed polystyrene particle suspensions were independent of the pore size and depended only on the surface porosity of MFI-UF membrane. The results showed that the membrane surface porosity decreased with MWCO from 10.5% (100 kDa) to 0.6% (5 kDa), and consequently the MFI-UF increased from 3700 to 8700 s/L^2, respectively. This increase in MFI-UF was attributed to the non-uniform distribution of membrane pores, which is exacerbated as surface porosity decreases. Consequently, preliminary correction factors of 0.4–1.0 were proposed for MFI-UF measured with UF membranes in the range 5–100 kDa. Finally, the surface porosity correction was applied to predict particulate fouling in a full-scale RO plant. However, additional research is required to establish correction factors for different types of feed water.

1. Introduction

Particulate fouling due to the deposition of particles/colloids on membrane surfaces is one of the problems experienced in many reverse osmosis (RO) membrane systems. Membrane fouling has several consequences, including: higher energy requirement and frequent membrane cleaning associated with increased use of chemicals and shorter membrane life [1]. Therefore, a method to assess, monitor and predict particulate fouling potential is really essential to optimize the performance of RO systems.

Currently, the most common methods used to assess particulate fouling potential are the Silt Density Index (SDI) and the Modified Fouling Index (MFI or MFI-0.45), which are standard methods in ASTM (under designation code: D4189 and D8002, respectively) [2,3]. The main advantage of the SDI is that it is simple to measure, even by non-professionals [4,5]. However, there have been growing doubts about its accuracy and reproducibility, attributed to the lack of correction factors for temperature, pressure and membrane resistance. Consequently, the SDI$^+$ was developed where the SDI value is corrected for the aforementioned parameters [6,7]. On the other hand, the MFI-0.45 has more advantages over the SDI as it is (i) derived based on cake/gel filtration, which is assumed to be the dominant particulate fouling mechanism in RO membranes, (ii) proportional to the particles concentration in feed water, and (iii) corrected for temperature and pressure [8]. The main drawback of the MFI-0.45 method is the use of a 0.45 μm membrane as a reference membrane to simulate the RO membrane. Hence, the particles/colloids smaller than 0.45 μm, which likely play a significant role in RO membrane fouling, are not considered in the method [9]. Consequently, the MFI-UF method was developed where an ultrafiltration (UF) membrane is used in order to capture smaller particles/colloids [10–14]. The MFI-UF method was initially performed at constant pressure (as the MFI-0.45). However, most of RO systems in practice operate at constant flux which is around 10–1000

* Corresponding author.IHE-Delft Institute for Water Education, Water Supply, Sanitation and Environmental Engineering Department, Westvest 7, 2611 AX, Delft, the Netherlands.
E-mail addresses: m.b.m.abunada@tudelft.nl, m.abunada@un-ihe.org (M. Abunada).

https://doi.org/10.1016/j.memsci.2022.120854
Received 10 April 2022; Received in revised form 30 June 2022; Accepted 20 July 2022
Available online 4 August 2022

Nomenclature

MFI-UF	Modified fouling index – ultrafiltration [s/L^2]
ΔP	Transmembrane pressure [bar or Pa]
J	Flux [L/m^2.h or m^3/m^2.s]
η	Feed water viscosity [N.s/m^2]
R_m	Clean membrane resistance [1/m]
I	Fouling index [1/m^2]
t	Filtration time [s, min, h, day, or month]
α	Specific cake resistance [m/kg]
C	Particle concentration [mg/L]
ε	Cake porosity [−]
ρ	Particle density [kg/m^3]
d	Particle diameter [m]
ΔP_o	Reference transmembrane pressure [= 2 bar or 200 kPa]
$\eta_{20°C}$	Reference water viscosity at 20 °C [= 0.001002 N s/m^2]
A_o	Reference MFI membrane surface area [= 0.00138 m^2]
Ω	Particle deposition factor [−]
R	RO recovery [−]
NDP	Net driving pressure [bar]
ΔNDP	Differential net driving pressure [bar]
Δx	MFI membrane thickness [m]
τ	MFI membrane tortuosity [−]
ε_m	MFI membrane surface porosity [−]
r_p	MFI membrane pore radius [m]
A_p	MFI membrane pore cross-sectional area [m^2]
N_p	Number of membrane pores [−]
A	MFI membrane geometric surface area [m^2]
V_{hc}	Cake hemisphere volume [m^3]
Q	Flow [m^3/s]

lower than the (initial) flux observed during the MFI-UF test at constant pressure. Therefore, the MFI-UF method was further developed to operate at constant flux filtration to more accurately simulate the operation of RO systems [15]. The MFI-UF at constant flux was primarily measured using hollow fibre UF membranes [15], while afterwards, it was further developed using flat-sheet membranes [16]. In addition, new methods were also introduced in the literature where the MFI-UF/MFI-0.45 method was further developed for better fouling assessment [17–22].

MFI-UF depends strongly on the molecular weight cut-off (MWCO) of the UF membrane used in the measurement. The lower the membrane MWCO, the smaller the membrane pore size, which allows the retention of smaller particles by the MFI-UF membrane and eventually results in a higher measured MFI-UF value [16]. Accordingly, assuming the particles retained on different MWCO membranes are equivalent in load and properties (i.e. same cake properties and thus same specific cake resistance on all membranes), then the measured MFI-UF value is assumed to be independent of the membrane MWCO. However, this might not be the case, as the measured MFI-UF value may also be affected by the membrane surface porosity. Membranes with low surface porosity and a non-uniform distribution of pores will have a smaller effective filtration area compared with their geometric filtration area. Hence, the local permeation flux through the cake formed on the surface of a membrane with a non-uniform porosity is expected to be higher [23,24]. Subsequently, this may cause the particles in the cake to be re-arranged, and simultaneously the cake can be compressed [25]. As a result, the cake resistance may increase, leading to a higher MFI-UF value for membranes with non-uniformly distributed pores.

Boerlage et al. [24] studied the effect of the surface porosity of hollow fibre polysulphone UF membranes on the MFI-UF measured at constant pressure filtration. The (field emission) scanning electron microscope (SEM) analyses showed that membranes with MWCO from 1 to 100 kDa (same manufacturer) had a similar range of surface porosities (2–6%), but the distribution of pores over the membrane surface appeared in different patterns. For the membranes ranging in MWCO from 10 to 100 kDa, the pores were distributed uniformly over the entire membrane surface. On the other hand, in the case of the membranes with MWCO from 1 to 5 kDa, the pores were only present on striations running lengthwise across the membrane surface. As a result, the MFI-UF measured using 1–5 kDa membranes was substantially higher than that obtained for the same feed water based on 10–100 kDa membranes. It was hypothesized that in the case of 1–5 kDa membranes, the cake formation might be limited to the porous striations only, while the remaining non-porous part of membrane surface was not involved in filtration and therefore ineffective. Consequently, this could result in a denser cake with higher resistance, which could eventually lead to (artificially) overestimated MFI-UF values. However, it was suggested that the effect of membrane surface porosity would be diminished if the MFI-UF test continued for longer duration (i.e. > 100 h), as the cake may eventually cover the entire membrane surface. Nevertheless, this was not verified in that study.

The effect of membrane surface porosity was also observed with microfiltration (MF) membranes in several studies [23,26–28]; where it was found that the rate of flux decline caused by cake/gel formation was faster when the membrane surface porosity was lower and non-uniformly distributed.

In addition, membrane surface porosity might also further decrease as a result of the influence of the membrane holder (housing) support which is placed underneath the membrane. This was reported by Nahrstedt and Camargo-Schmale [29] and Salinas Rodriguez et al. [30] during the measurement of MFI-0.45 using several holder supports with different permeable surface areas. It was found that the non-permeable part of the holder support could block membrane pores which were directly in contact with the support. Consequently, it was found that the smaller the permeable surface area of the holder support, the lower the membrane surface porosity, the smaller the effective filtration area, and eventually the higher the measured MFI-0.45 value.

Although the studies reviewed above suggested/hypothesized the effect of membrane surface porosity on particulate fouling, the effect was not proven experimentally. In addition, the studies did not propose nor describe a method to measure and quantify the effect of membrane surface porosity. Moreover, the aforementioned studies focused on constant pressure filtration using mostly MF membranes, while the latest developments of the MFI-UF method utilize UF membranes operating at a constant filtration flux.

Therefore, the aim of this study was to verify and quantify the effect of membrane surface porosity on the MFI-UF measured at constant flux to improve particulate fouling prediction in RO systems. Flat-sheet polyethersulfone (PES) UF membranes with MWCO of 5, 10, 50 and 100 kDa were examined. The following research objectives were investigated:

(1) To characterize the UF membranes used to measure the MFI-UF (5–100 kDa) in terms of their surface porosity and the distribution of pores across the surface using ultra-high resolution SEM.
(2) To demonstrate (theoretically) the effect of membrane surface porosity on the effective filtration area during the MFI-UF test.
(3) To develop an approach to quantify the effect of surface porosity on the MFI-UF measured with 5–100 kDa membranes. To achieve this, it was essential to ensure complete retention of particles on the 5–100 kDa membranes during the MFI-UF measurements in order to eliminate the effect of membrane pore size on the

measured MFI-UF (i.e. to quantify the membrane surface porosity effect, the measured MFI-UF should be independent of the pore size and depend only on the surface porosity of the membranes).
(4) To identify whether the membrane holder support used in MFI-UF test affects the membrane surface porosity and thus the measured MFI-UF.
(5) To illustrate the effect of surface porosity of MFI-UF membrane on particulate fouling prediction in a full-scale RO plant.

2. Background: MFI-UF constant flux

MFI-UF was derived based on cake/gel filtration [15]. At constant flux, cake/gel filtration can be defined by the linear relationship between the transmembrane pressure (ΔP) and filtration time (t), as described by Equation (1).

$$\Delta P = J.\eta.R_m + J^2.\eta.I.t \quad (1)$$

where J is the flux rate, η is the feed water viscosity, R_m is the clean membrane resistance, and I is the fouling index which describes the fouling potential of feed water.

The fouling index (I) is defined by the product of the specific cake resistance (α) and particle concentration in feed water (C), as shown in Equation (2).

$$I = \alpha.C \quad (2)$$

Specific cake resistance (α) can be defined according to the Carman-Kozeny equation [31] as a function of the porosity of the cake formed on the membrane surface (ε), particle diameter (d) and particle density (ρ), as shown in Equation (3).

$$\alpha = \frac{180.(1-\varepsilon)}{\rho.d^2.\varepsilon^3} \quad (3)$$

During the MFI-UF test, transmembrane pressure increases over time, typically, in three subsequent mechanisms, as shown in Fig. 1; (i) pore blocking (plus system start-up), (ii) cake/gel filtration, and (iii) cake/gel compression.

First, the value of I is determined from the slope of the linear phase of cake/gel filtration, as shown by Equation (4).

$$I = \frac{1}{J^2.\eta}.slope \quad (4)$$

Then the MFI-UF, by definition, is determined based on I value and corrected to the reference testing conditions proposed by Schippers and Verdouw [8], as shown in Equation (5).

$$MFI\text{-}UF = \frac{\eta_{20^\circ C}.I}{2.\Delta P_o.A_o^{\,2}} \quad (5)$$

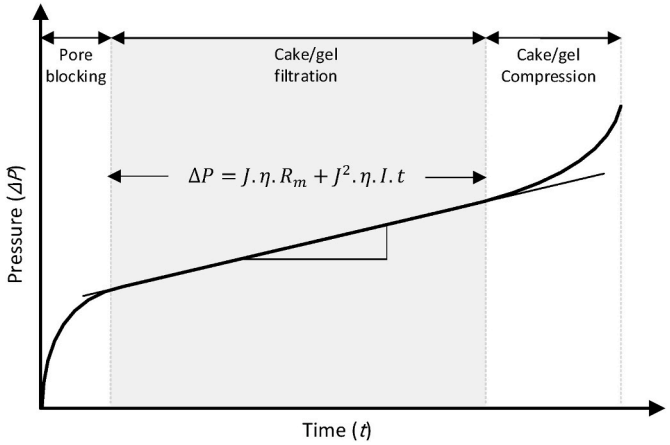

Fig. 1. Typical filtration curve during an MFI-UF test at constant flux.

where ΔP_o, $\eta_{20^\circ C}$ and A_o are the reference pressure, water viscosity and membrane surface area, respectively [8].

MFI-UF can be also described by combining Equations (2), (3) and (5), as shown in Equation (6).

$$MFI\text{-}UF = \frac{90.\eta_{20^\circ C}.(1-\varepsilon).C}{\Delta P_o.A_o^{\,2}.\rho.d^2.\varepsilon^3} \quad (6)$$

The MFI-UF value can be used as an input in the model shown by Equation (7) to predict the particulate fouling rate in RO plants. The fouling rate is described by the increase in the net driving pressure (ΔNDP) due to the cake/gel formation on RO membrane, assuming no contribution by concentration polarization, scaling and biofouling [32].

$$\frac{\Delta NDP}{t} = \frac{2.\Delta P_o.A_o^2.J^2.\eta.\Omega.MFI\text{-}UF}{\eta_{20^\circ C}} \quad (7)$$

since the MFI-UF is performed at dead-end filtration, the particles deposition factor (Ω) is incorporated in the prediction model to simulate the portion of particles depositing on RO membrane under cross-flow filtration. The deposition factor can be measured using Equation (8), based on the MFI-UF of RO feed, MFI-UF of RO concentrate and RO recovery rate (R). Ideally, the Ω value may vary between 0 and 1; where $\Omega = 0$ indicates no particle deposition, and $\Omega = 1$ indicates that all particles existed in the water passing the RO membrane deposited and remained on its surface [16].

$$\Omega = \frac{1}{R} + \frac{MFI\text{-}UF_{concentrate}}{MFI\text{-}UF_{feed}}.\left(1-\frac{1}{R}\right) \quad (8)$$

3. Materials and methods

3.1. MFI-UF measurement

MFI-UF measurements were performed using the set-up presented in Fig. 2. The set-up consisted of three main components: (i) infusion syringe pump (PHD ULTRA ™, Harvard Apparatus, USA), (ii) pressure transmitter (PXM409, Omega, USA), and (iii) membrane holder (Whatman®, USA) where the UF membrane was placed. Feed water was infused by the pump and filtered through the membrane at constant flow. Pump flow (Q) was set based on the membrane surface area (A) and the required flux rate (J), where $Q = J.A$. The data of ΔP vs t was recorded by the pressure transmitter and transferred to the connected computer. Finally, the MFI-UF value was calculated based on Equations (4) and (5).

3.2. MFI-UF membranes

The pore size of the MFI-UF membrane should be smaller than the particles in the feed water to be assessed. In RO filtration, the size range of particles that deposit on the RO membrane is not known. Therefore, in this study, a wide range of MWCOs was investigated for MFI-UF; 5, 10, 50, and 100 kDa. The selected UF membranes were made of polyethersulfone (PES), and had flat-sheet configuration with a surface diameter of 25 mm (Biomax®, Millipore, USA). All membranes were pre-cleaned by filtering at least 100 mL of ultra-pure water (Milli-Q®, Millipore, USA) at a constant flux of 200–300 L/m^2.h to remove preservation chemicals.

Membrane resistance (R_m) was measured prior to the MFI-UF measurement, to verify that the membranes are manufactured consistently and not damaged. R_m can be described by the Hagen-Poiseuille equation (Equation (9)) as a function of membrane thickness (Δx), tortuosity (τ), surface porosity (ε_m) and pore radius (r_p).

$$R_m = \frac{8.\Delta x.\tau}{\varepsilon_m.r_p^{\,2}} \quad (9)$$

however, since the parameters above are not provided by the manu-

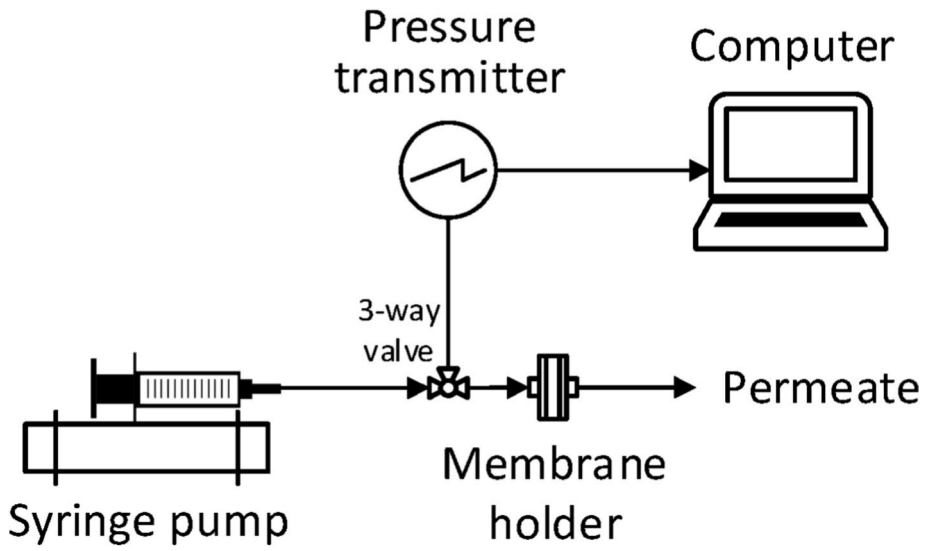

Fig. 2. Scheme of MFI-UF set-up at constant flux filtration mode.

facturer, R_m was measured experimentally by filtering ultra-pure water (Milli-Q) at constant flux, and then, R_m value was calculated using Equation (10).

$$R_m = \frac{\Delta P}{J.\eta} \tag{10}$$

3.3. Characterization of MFI-UF membrane surface

The surface of MFI-UF membranes was characterized using ultra-high resolution SEM (FEI Magellan 400) at magnification of 500,000x and accelerated voltage of 3 kV. The images generated by the SEM were further processed using ImageJ software to identify the surface porosity and the distribution of pores over the membrane surface.

3.4. Theoretical demonstration of membrane surface porosity effect during the MFI-UF testing

According to Boerlage et al. [24], the effect of membrane surface porosity on the effective filtration area and thus on the measured MFI-UF may be expected to diminish if the duration of the MFI-UF test is very long. To demonstrate this, it was first important to understand how the cake develops on the membrane surface in relation to the uniformity of the membrane surface porosity.

It was hypothesized that the cake development on the membrane surface during the MFI-UF test progresses as shown in Fig. 3. Just after pore blocking, the particles start to accumulate over and around the pores forming separated mounds of particles on the membrane surface (Fig. 3 (a)). These mounds continue growing in a form of cake hemispheres which will expand on the membrane surface until they overlap (Fig. 3 (b)). Consequently, continuous and even cake layers will eventually start to build up over the entire membrane surface (Fig. 3 (c)).

Based on the hypothesis above, the extent of the effect of membrane surface porosity was theoretically (i.e. non-experimentally) determined by calculating the approximate time required until the stage where the membrane surface area is completely covered by cake is reached, and thus the total area becomes effective in filtration (i.e. once the cake hemispheres overlap). Membrane pores were assumed to be uniformly distributed over the membrane surface (i.e. the distance between all membrane pores is identical).

Firstly, it was assumed that all membrane pores have the same size. Accordingly, the number of pores (N_p) was calculated by dividing the porous area by the average cross-sectional area of 1 membrane pore (A_p), where the porous area is the product of the membrane surface porosity (ε_m) and total membrane surface area (A), as shown in Equation (11).

$$N_p = \frac{\varepsilon_m.A}{A_p} \tag{11}$$

Secondly, it was assumed that one cake hemisphere develops over each membrane pore. In addition, the developed hemispherical cake was assumed to be non-porous and incompressible. Hemisphere volume (V_{hc}) development was calculated by dividing the total cake volume over time by the number of pores (N_p). Where the total cake volume over time was calculated by the product of the feed flow (Q) and particles concentration in the feed (C) divided by particles density (ρ), as shown in Equation (12). Particles were assumed to be equivalent in density to the polystyrene particles ($\rho = 1.05$ g/cm^3).

$$V_{hc} = \frac{Q.C}{\rho}.\frac{1}{N_p}.t \tag{12}$$

Thirdly, based on the hemisphere volume, the hemisphere base area could be calculated over time. Accordingly, the hemispheres will cover the entire membranes surface once the summation of hemisphere base areas is equal to the total membrane surface area. At this stage, it is considered (theoretically) that the filtration area becomes stable over time and no longer impacted by the surface porosity of the membrane.

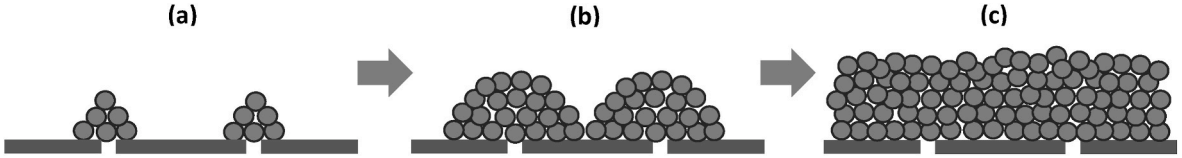

Fig. 3. Schematic diagram illustrating the hypothesized cake development on the membrane surface during MFI-UF test; (a) separated mounds, (b) overlapping hemispheres, and (c) continuous/even layers.

3.5. Approach to quantify the effect of membrane surface porosity on the measured MFI-UF

The theoretical demonstration of the effect of membrane surface porosity addressed in the previous section (3.4) was assessed experimentally by measuring the MFI-UF using different UF membranes (5, 10, 50 and 100 kDa).

A new approach was proposed to ensure complete retention of particles by the 5–100 kDa membranes during the MFI-UF test. Complete particle retention is a prerequisite in order to ensure that the load of particles (and properties of cake) retained on all membranes are identical. Consequently, any difference in the measured MFI-UF can be attributed to the variation in surface porosity of the investigated membranes. In case complete retention of particles is not achieved, then the observed differences in the measured MFI-UF can also be as a result of the variation in particle retention due to the different pore sizes of the UF membranes.

Fig. 4 shows the approach followed to ensure complete particle retention. The MFI-UF was measured for a feed suspension of particles in ultra-pure water (Milli-Q) using 5–100 kDa membranes. Assuming that all particles were retained on the 5–100 kDa membranes (stage 1), then the measured MFI-UF of the permeates (stage 2) should be similar to the MFI-UF of ultra-pure water which is below the limit of detection (LOD) value; $\approx 200\ s/L^2$ (LOD measurement is presented in Appendix A). All MFI-UF measurements were performed at a constant flux of 100 $L/m^2.h$.

3.5.1. Preparation of feed samples used to quantify the effect of membrane surface porosity

The feed sample was initially prepared using monodisperse polystyrene particles (Bangs Laboratories, USA). Polystyrene particles were the preferred choice to verify surface porosity based on several criteria, including; (i) polystyrene particles are inert and are chemically very stable [33], (ii) feed suspensions are easy to prepare (just by diluting the manufactured polystyrene suspension with ultra-pure water), (iii) polystyrene particles are commercially available and relatively inexpensive (price in 2020 was 200 Euro per 1.5 g of 10% concentration), and (iv) polystyrene particles have been used in particulate fouling tests by several researchers [34–40]. The selected polystyrene particles had a nominal size of 75 nm. Based on the technical manufacturing data sheet (in Appendix B), the particle size range (65–85 nm) was larger than the pore size range of the 5–100 kDa membranes (which were characterized by ultra-high resolution SEM in advance). Particles with a size significantly larger than the MWCO of the selected membranes were considered unsuitable as large particles are not expected to affect the MFI-UF considerably (since the MFI-UF is inversely proportional to the square of particle size, as shown in Equation (6)), and thus the effect of membrane surface porosity variation on the measured MFI-UF would not be noticeable in this case.

Preliminary investigations showed that feed suspension prepared with polystyrene particles could not ensure the criterion of complete particle retention, as the MFI-UF values of the collected permeates were considerably higher than the MFI-UF of ultra-pure (i.e. $\gg$ LOD), as shown in Fig. 5 (a). This means that the particle load (i.e. the specific cake resistance) on the 5–100 kDa membranes (stage 1) was different and thus the difference in the measured MFI-UF could not be attributed to the effect of membrane surface porosity only but also to the different retention of polystyrene particles achieved with each membrane. Based on the manufacturer's information, the high MFI-UF values measured for the UF permeates were mainly attributed to the existence of some small particle fractions and/or surfactant residual in the prepared suspensions, such that these small components could partially pass through the 5–100 kDa membranes (in stage 1) but probably were retained on the subsequent 5 kDa membranes (in stage 2) due to particle bridging [41].

In further trials, silver particles of 80 nm (Sigma-Aldrich, USA) and pullulan particles of 800 kDa (Sigma-Aldrich, USA) were also tested, both of which were larger than the pore size range of the 5–100 kDa membranes examined in this study (technical data sheets of both silver and pullulan particles are in Appendix B). Silver particles were selected as they are assumed to be more rigid and have less affinity to be fractured in comparison with polystyrene particles. Whereas, the pullulan particles are used as they are a standard reference material (for calibration in chromatography) and have a well-defined structure [42]. Thus, for both particle types, negligible small particle fractions were expected in the prepared feed samples. Nevertheless, preliminary investigations showed that the feed samples prepared by both types of particles could not be completely retained on the 5–100 kDa membranes and thus full particle retention was not achieved, as shown in Fig. 5 (b) and (c). The reason was also mainly attributed to the presence of small particle fractions which might have already existed in the supplied particles and/or were created during sample preparation.

Therefore, it was concluded that none of the commercially available particles tested in this study were suitable to be used as supplied, and an approach was developed to pre-wash the particles to remove the surfactant and the associated particle fractions that were smaller than the pore size of the 5–100 kDa membranes. In this study, particle washing was only investigated for the polystyrene particles, as they were considerably less expensive than the other particles (pullulan and silver).

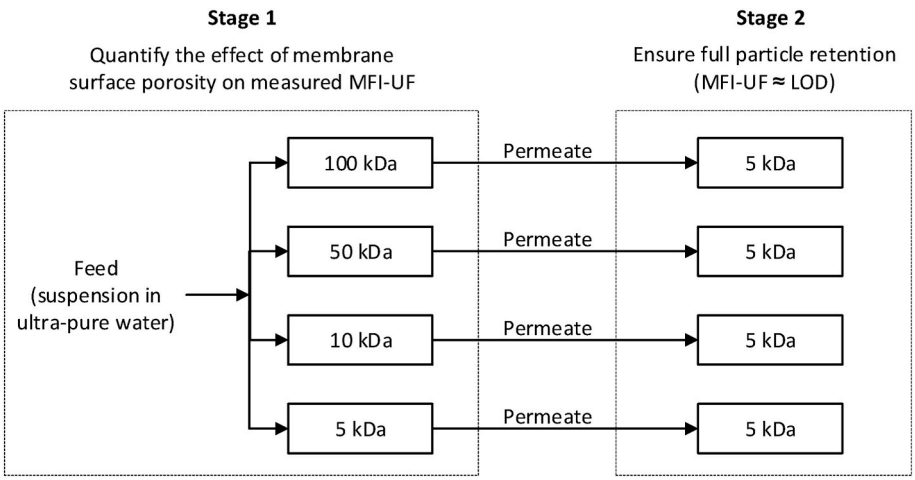

Fig. 4. The newly developed approach to verify the effect of membrane surface porosity on the MFI-UF measured at constant flux.

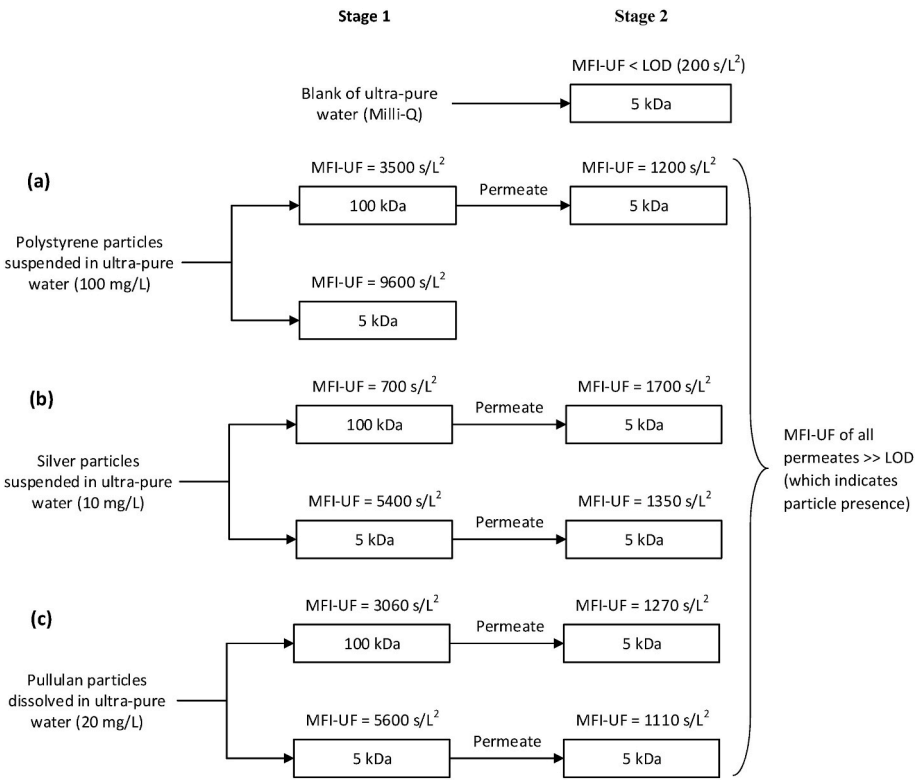

Fig. 5. Preliminarily investigation to verify the effect of membrane surface porosity on measured MFI-UF using feed solution/suspension of (a) unwashed polystyrene particles (75 nm), (b) silver particles (80 nm), and (c) pullulan particles (800 kDa).

3.5.2. Washing of polystyrene particles to remove surfactant and small particle fractions

The objective of polystyrene particle washing was to remove the small particle fractions and residual surfactant (sodium dodecyl sulphate) created or added during the manufacturing process. For this purpose, several particle washing techniques were investigated; centrifugation, dialysis, unstirred dead-end filtration and stirred dead-end filtration, where the efficiency of each technique was evaluated based on the approach described in Fig. 4. Eventually, the stirred dead-end filtration, which was the most promising washing technique, yielded complete retention of the polystyrene particles (the results of all washing experiments are addressed in detail in Appendix C).

Polystyrene particles were washed by stirred filtration, as shown in Fig. 6; using a 200 mL dead-end stirred cell (Amicon®, Millipore, USA) equipped with a 500 kDa PES membrane (Biomax®, Millipore, USA). The MWCO of the cell membrane (500 kDa) was selected so that small particle fractions and surfactant in the polystyrene particle suspension could pass through while retaining only the larger particles (>500 kDa). Thus, this ensures that the washed particles (i.e. retained on the 500 kDa membrane) should be completely retained on the 5–100 kDa membranes. The washing procedure was as follows.

1. A prepared suspension of polystyrene particles (200 mg/L) was placed in the Amicon cell.
2. The connected pressure vessel was filled with ultra-pure water (Milli-Q).
3. The stirred filtration of the polystyrene suspension was started simultaneously while filling the cell with ultra-pure water from the pressure vessel (i.e. the inflow of ultra-pure water in the cell = the outflow of filtrate from the cell). Hence, during filtration, the polystyrene particles were washed (by the ultra-pure water) while small

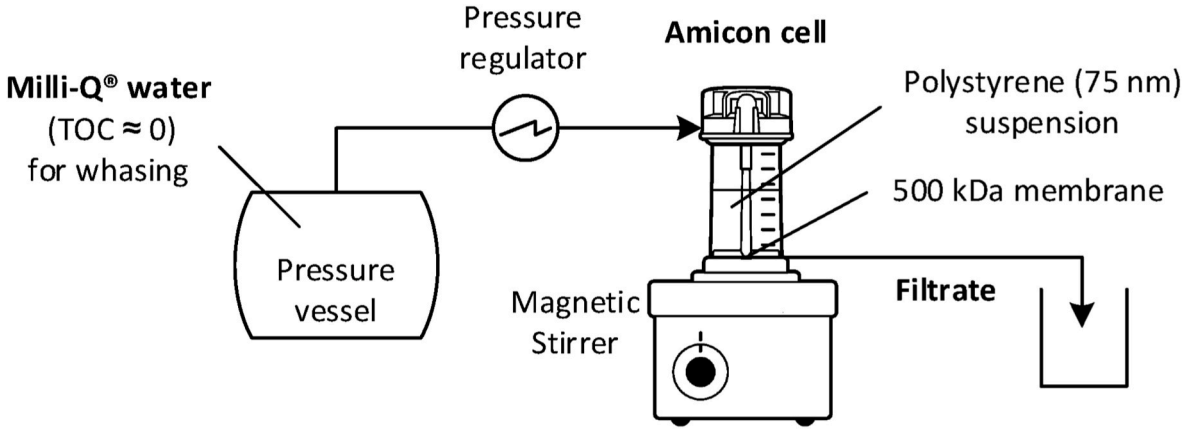

Fig. 6. Polystyrene particle washing approach using stirred UF filtration at constant pressure.

fractions of particles as well as surfactant were filtered through the 500 kDa membrane.
4. The total organic carbon (TOC) of the filtrate was measured during filtration (every 30 min).
5. The filtration was stopped once the TOC of the filtrate equalled that of the ultra-pure water (TOC <0.2 mg/L), which confirmed that most small fractions and surfactant were filtered through the 500 kDa membrane. Thereby, the suspension remaining in the cell after filtration comprised washed polystyrene particles (larger than 500 kDa).
6. The washed particle suspension which remained in the cell was then used to quantify the effect of membrane surface porosity (Fig. 4) on the MFI-UF. The concentration of washed polystyrene particles was estimated by measuring the TOC of the suspension, where the percentage of carbon in polystyrene $(C_8H_8)_n$ is 92%. Accordingly, the washed polystyrene concentration equalled TOC/0.92.

Particle washing by stirred filtration was initially investigated at a constant pressure of 250 mbar. In this scenario, the washing process lasted for around 6 h, and at that point the TOC of the filtrate was <0.2 mg/L, which was the criterion indicating that washing was complete. However, in many cases, washing was insufficient since the feed suspension of washed polystyrene particles did not satisfy the criterion of complete particle retention described in Fig. 4 (stage 2), whereby the MFI-UF of the permeate was considerably higher than the target value (results are presented in Appendix C). The reason was attributed to pore blocking of the Amicon cell membrane (500 kDa) which could restrict part of the small particle fractions and surfactant from passing through the 500 kDa membrane.

Consequently, washing was enhanced by performing the stirred filtration at a lower pressure of 100 mbar to reduce the flux rate and thus minimize membrane pore blocking. In addition, the 500 kDa membrane in the Amicon cell was replaced twice during the washing process (i.e. 3 membranes were used in total), where steps 1–5 mentioned above were repeated after each membrane replacement. The overall washing process required around 8 h. Particle washing conducted under these conditions (i.e. at 100 mbar using 3 different 500 kDa membranes in the Amicon cell for a period of 8 h) was successful and satisfied the criterion of complete particle retention (Fig. 4 (stage 2)), and the MFI-UF values of all UF permeates were less than the LOD (<200 s/L^2) as shown in Fig. 7.

3.6. Identification of membrane holder support effect on the membrane surface porosity

The effect of the membrane holder support pad on membrane surface porosity and thus on the measured MFI-UF was investigated using the membrane holder support shown in Fig. 8 (Whatman®, USA). The support pad had two sides with different surface engravings; channels (Fig. 8 (a)) and perforations (Fig. 8 (b)). The ratio of the permeable area to the total surface area of the pad was around 50% and 25% for the channelled and perforated sides, respectively.

The effect of the support pad on the membrane surface porosity was investigated by measuring and comparing the clean resistance (R_m) measured with each side of the pad. This was done for the 10 kDa membrane (low MWCO) and 100 kDa membrane (high MWCO), at a constant flux of 200 L/m^2.h (using Equation (10)). Four replicated measurements were carried out with each pad side.

Based on Equation (9), R_m is inversely proportional to the membrane surface porosity. Therefore, in case contact between the support pad and the membrane blocks some membrane pores and thus reduces the surface porosity, then it is expected that the R_m measured based on the perforated side should be higher than that of the channelled side (since the non-permeable part of the perforated side is higher, and thus the possible reduction in membrane surface porosity due to pore blocking is expected to be higher).

3.7. Applying the MFI-UF to predict particulate fouling in a full-scale RO plant – with and without a correction for the surface porosity of the MFI-UF membrane

To illustrate the effect of surface porosity of the MFI-UF membrane, the MFI-UF was applied to predict the particulate fouling rate in a full-scale RO drinking water treatment plant. The RO plant produces drinking water from surface water with conventional pre-treatment processes, comprising micro strainers, coagulation, sedimentation, rapid sand filtration and granular activated carbon filtration, followed by 150 kDa UF membranes, and then 2-stage RO membranes. Water samples were collected from the RO feed and RO concentrate of the first stage ($J = 26$ L/m^2.h, $R = 57\%$). Table 1 shows the general water quality parameters of the collected RO feed samples.

The MFI-UF of the collected RO feedwater and concentrate samples was measured using 5–10 kDa membranes at the same flux rate applied

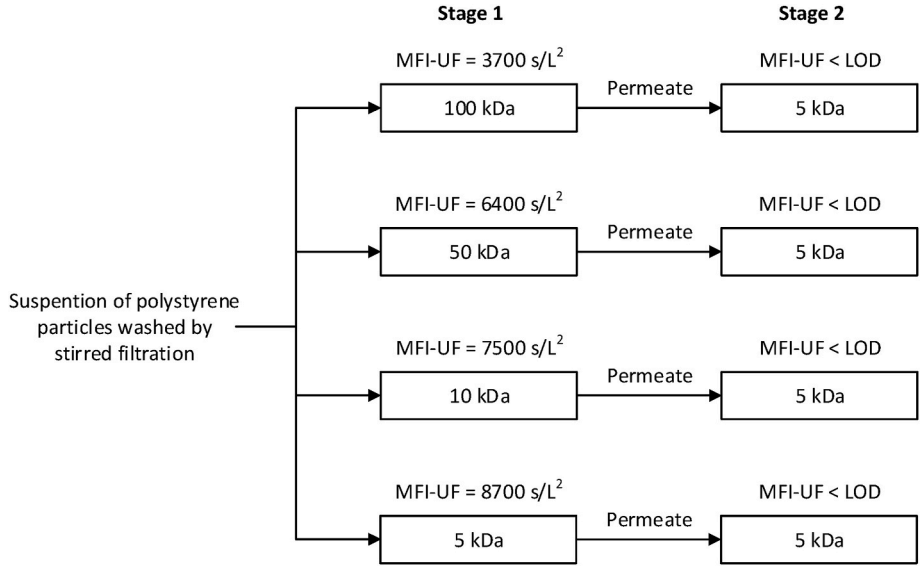

Fig. 7. The effect of non-uniform membrane surface porosity on the MFI-UF using a suspension of polystyrene particles washed by stirred dead-end filtration (Amicon cell).

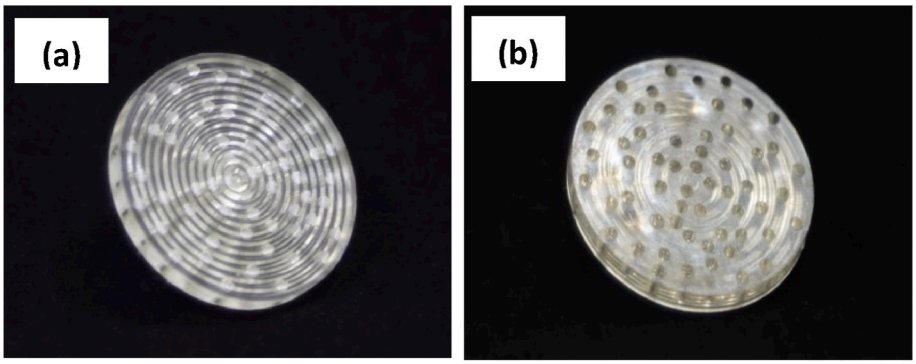

Fig. 8. Membrane holder support pad; (a) channelled side, and (b) perforated side.

Table 1
Characteristics of RO feed at collection time.

Parameter	Value	Parameter	Value
Cations:		Anions:	
Calcium	58.2 mg/L	Carbonate	<5 mg/L
Magnesium	13.6 mg/L	Chloride	160 mg/L
Sodium	82.4 mg/L	Silica	1.6 mg/L
Iron	<0.005 mg/L	Sulphate	68 mg/L
Barium	0.04 mg/L	Bicarbonate	149 mg/L
Strontium	0.40 mg/L		
Other parameters:			
Temperature	5 °C	EC	0.85 mS/cm
pH	8	DOC	2.6 mg/L

in the RO plant (26 L/m^2.h). Subsequently, the deposition factor (Ω) was determined (Equation (8)), and the NDP increase rate was predicted (Equation (7)) for each MFI-UF membrane. Finally, the agreement between the NDP increase rate observed in the plant and the NDP increase rate predicted based on the MFI-UF was assessed both with and without the correction for the effect of the surface porosity of the MFI-UF membranes (based on the outputs of the investigation addressed in the previous sections (3.3-3.6)).

4. Results and discussion

4.1. Membrane surface characterization – SEM analysis

Fig. 9 presents the images of the surface of the 5, 10, 50 and 100 kDa membranes scanned by ultra-high resolution SEM (at a magnification of 500,000x). One important remark is that the pore openings shown in the

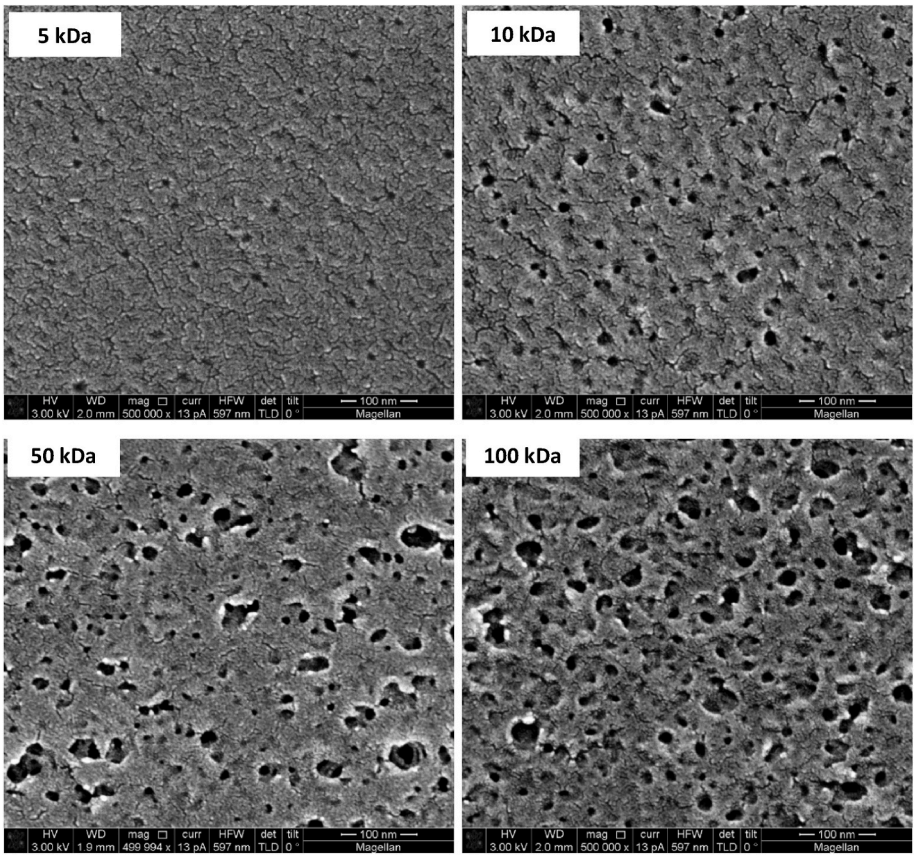

Fig. 9. Ultra-high resolution SEM images of the surface of 5–100 kDa PES membranes (magnification of 500,000x).

SEM images might be narrowed or blocked just underneath the membrane surface. Therefore, the porous area scanned by SEM might be even smaller than in reality. Accordingly, the measurements of membrane surface porosity and pore size distribution were considered as an indication and not as absolute figures.

Based on the SEM images, it was observed that the lower membrane MWCO, the lower the membrane surface porosity as well as the more the pores are non-uniformly distributed over membranes surface. All membranes in general had low surface porosity; 0.6, 2.9, 6.1 and 10.5% for 5, 10, 50 and 100 kDa membrane, respectively.

The relationship between the membrane MWCO and the measured surface porosity was found to be logarithmic in the studied range, as shown in Fig. 10. This means that the difference in surface porosity is major at lower MWCOs, while it becomes less in the higher MWCO range. For instance, the difference in surface porosity between a 5 and 10 kDa membrane is a factor of 5 times, while the difference between a 95 and 100 kDa membranes is nearly negligible. This can be supported visually based in the SEM images (Fig. 9), where the difference in the surface porosity decreases markedly when the MWCO increases.

Fig. 11 shows the pore size distribution of the 5–100 kDa membranes based on a scanned area of 1 μm^2 (the pore size is the equivalent diameter assuming the cross-sectional area of the pore is circular). As it can be observed, the higher the membrane MWCO, the wider the pore size distribution. However, more than 60–80% of pores were within the size range of 6–12 nm. In addition, the mean pore size was similar for all membranes; 8.0, 9.2, 10.1 and 10.6 nm for 5, 10, 50 and 100 kDa membrane, respectively.

4.2. Theoretical effect of membrane surface porosity during the MFI-UF testing

Fig. 12 shows the theoretical time required until the membrane surface area is completely covered by a particle-cake during an MFI-UF test, such that the effective filtration area is independent of the membrane surface porosity. The time was calculated assuming that membrane pores are uniformly distributed over the surface. This was done based on the steps explained in section 3.4, using the measured membrane surface porosity and mean pore size characterized by ultra-high resolution SEM (section 4.1). As can be observed, the extent of the effect of membrane surface porosity was inversely correlated to the membrane MWCO (i.e. surface porosity as well). This is because the formed cake hemispheres (Fig. 3 (b)) require more time to overlap and cover the entire membrane surface in case the interspacing between the membrane pores was larger (due to lower surface porosity).

In addition, the theoretical calculations showed that the effect of membrane surface porosity is highly dependent on the flux rate applied in the MFI-UF test. This is because the lower the flux, the lower the load

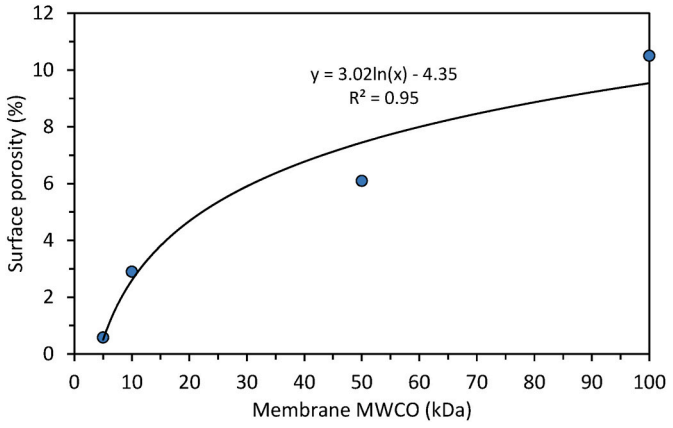

Fig. 10. Relationship between membrane MWCO and surface porosity based on ultra-high resolution SEM analysis.

of particles depositing on the membrane surface over time, thus requiring more time for the particle-cake to cover the entire membrane surface. Accordingly, in Fig. 12, since the difference between the flux of 20 L/m^2.h (left Y-axis) and 100 L/m^2.h (right Y-axis) is to a factor of 5, thus the calculated time required until the particle-cake covers the entire membranes surface at a flux of 20 L/m^2.h was 5 times longer than that at 100 L/m^2.h.

Moreover, based on Fig. 12, the effect of membrane surface porosity appeared to dramatically decrease when the particle concentration increased (particularly at the concentration range of 1–5 mg/L), where the cake formation takes relatively shorter time to cover the entire membrane surface since the load of particles depositing on membrane surface over time becomes higher. In the worst-case studied scenario; at 1 mg/L concertation, 5 kDa membrane and 20 L/m^2.h flux rate, the effect of membrane surface porosity would last for around 110 min. Whereas this duration decreases to 22 min when the particle concentration increases to 5 mg/L. Based on this theoretical calculation (Fig. 12), it could be suggested that if the MFI-UF test was carried out for prolonged periods of time, then the measured MFI-UF value would be (theoretically) independent of the membrane surface porosity (i.e. the effect of membrane surface porosity is temporary and diminishes in time as long as the MFI-UF test lasts long enough for a particle-cake to form on the entire membrane surface).

4.3. Quantifying the effect of membrane surface porosity on the measured MFI-UF

Fig. 13 shows the MFI-UF of the feed suspension of washed polystyrene particles measured at a constant flux of 100 L/m^2.h, using a range of membranes (5, 10, 50 and 100 kDa) with different surface porosities. Complete particle retention was verified with all membranes, as shown in Fig. 7. This means that the observed increase in the MFI-UF values could be attributed to the reduction in the surface porosity of the membrane and was independent of the membrane pore size. The measured MFI-UF value was linearly correlated to the membrane surface porosity, where the MFI-UF increased by around 500 s/L^2 per 1% decrease in the membrane surface porosity. However, by extrapolating the regression line, the MFI-UF value will approach zero at higher surface porosity (18.3%), which is not possible. This means that the correlation between the MFI-UF and membrane surface porosity observed in Fig. 13 is probably valid only in the studied range, while the correlation at higher surface porosities (>10.5%) should be further investigated.

However, the result of the MFI-UF dependency on the membrane surface porosity shown in Fig. 13 is in conflict with the theoretical calculation illustrated in section 4.2. Whereas, based on Fig. 12, the effect of membrane surface porosity should have diminished after less than 1 min of cake filtration at the same flux (100 L/m^2.h) and particle concentration (the concentration was 65 mg/L after polystyrene particles washing). Nevertheless, the effect of membrane surface porosity on the (experimentally measured) MFI-UF shown in Fig. 13 was still observed although the duration of the MFI-UF tests was longer than 60 min.

The reason for this contradiction was attributed mainly to the pattern of surface porosity; i.e. the uniformity of pore distribution over the membrane surface. In the theoretical calculation, the pores were assumed to be identical in size and uniformly distributed over the membrane surface (equal inter-pores spacing). As it can be observed from Fig. 9, the pore distribution shows non-uniformity across the membrane surface; with extensive areas of the membrane surface being completely non-porous and other regions showing the presence of pores. This is exacerbated as the membrane MWCO decreases (mostly observed with the 5 and 10 kDa membrane). Consequently, cake formation might be permanently limited to the porous regions only, as illustrated in the schematic diagram in Fig. 14 (left). In this case, the effective filtration area (A_{eff}) of the membrane is less than the geometric surface area (A) of

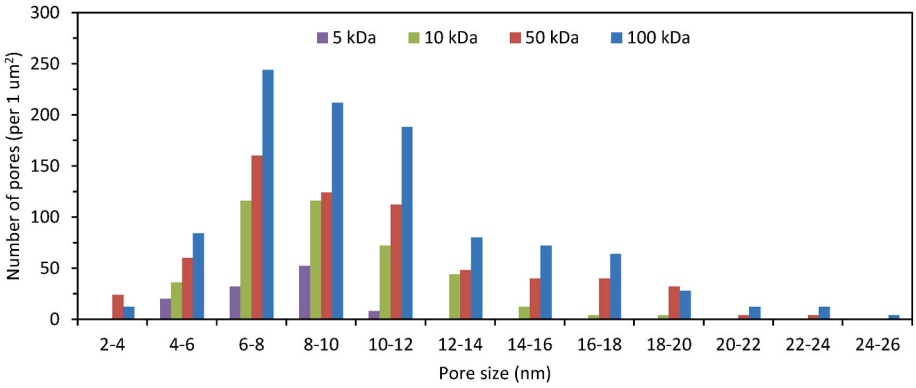

Fig. 11. Pore size distribution of 5–100 kDa membranes based on ultra-high resolution SEM analyses.

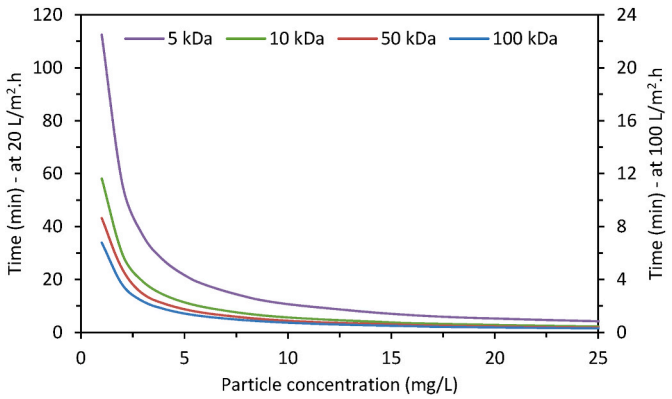

Fig. 12. Time required until membrane surface is entirely covered by cake, assuming that the membrane pores are uniformly distributed over the surface.

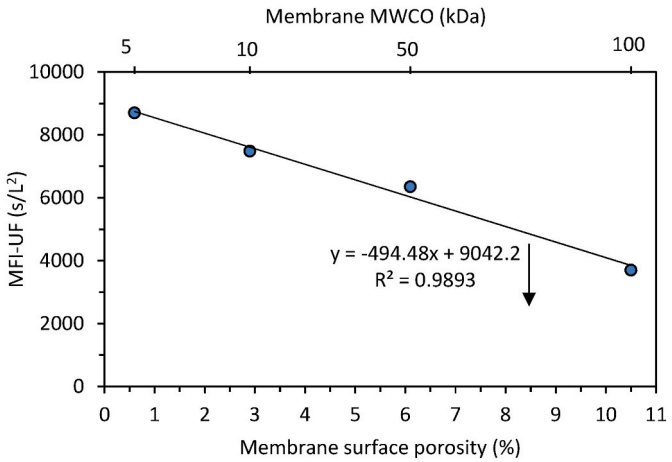

Fig. 13. Relationship between MFI-UF of washed polystyrene particles suspension, membrane surface porosity and membrane MWCO.

the membrane. Subsequently, at constant pump flow (Q), the actual local flux through the formed cake (i.e. Q/A_{eff}) will be higher than that when the cake is evenly distributed over the entire membrane surface (Fig. 14 (right)), which will eventually result in higher (i.e. overestimated) MFI-UF.

According to the above explanation illustrated in Fig. 14 and based on the results shown in Figs. 9 and 13, it could be concluded that the lower the membrane MWCO, the lower the membrane surface porosity, and the more non-uniformly the membrane pores are distributed and the greater the distance between the pores. Thus, this resulted in smaller effective membrane filtration area, and subsequently higher local flux, which eventually led to overestimation of the MFI-UF.

4.3.1. *Correcting the effect of membrane surface porosity on the measured MFI-UF*

In order to eliminate the effect of membrane surface porosity, the measured MFI-UF of polystyrene suspension had to be corrected based on a reference/standard MFI-UF value where the effect of non-uniform membrane surface porosity is very low/negligible. Ideally, a theoretical reference MFI-UF value for the polystyrene particle suspension should have been calculated (using Equation (6)) where no effect of membrane surface porosity (i.e. cake covers the entire membrane surface) existed. However, since the porosity of the cake formed on membrane surface is not known, the MFI-UF of the polystyrene particle suspension cannot be theoretically calculated from first principles (using Equation (6)). Consequently, the reference MFI-UF had to be find experimentally. Based on the available ultra-high resolution SEM images (Fig. 9), the 100 kDa membrane was identified as the membrane with the most uniformly distributed pores over membrane surface as well as with the shortest distance between membrane pores. Accordingly, it was expected that the effect of non-uniform surface porosity is low with this membrane. Therefore, the MFI-UF measured based on 100 kDa membrane was chosen as a reference to correct the effect of surface porosity of the other UF membranes with lower MWCO (and lower surface porosity). Nevertheless, the selection of a 100 kDa UF membrane as a reference should be further investigated (using a technique other than ultra-high resolution SEM) to prove that the distribution of pores is indeed uniform across the membrane.

Since the MFI-UF increase due to the effect of membrane surface porosity was linear (Fig. 13), the MFI-UF values were corrected linearly in relation to the MFI-UF of a 100 kDa membrane. Accordingly, the identified correction factors are shown in Table 2. For example, the correction factor for the 5 kDa membrane = $\text{MFI-UF}_{5\text{ kDa}}/\text{MFI-UF}_{100\text{ kDa}}$ = 3700/8700 s/L^2 = 0.4.

4.4. *Effect of membrane holder support on membrane surface porosity*

Fig. 15 shows the R_m of the 10 and 100 kDa membranes, measured with each side of the membrane holder support pad (Fig. 8). As can be observed for each membrane MWCO, the average measured R_m was very similar for both sides of the support pad despite the major difference in the permeable area of the two sides (factor of 2). This could indicate that neither side of the support pad had any influence on membrane surface porosity and thus on the measured MFI-UF.

However, the result discussed above is in contrast with the findings of Nahrstedt and Camargo-Schmale [29] and Salinas Rodriguez et al. [30], where a strong effect was observed due to the membrane holder support pad on the surface porosity of a 0.45 μm MF membrane. The main reason can be attributed to the difference in the cross-sectional

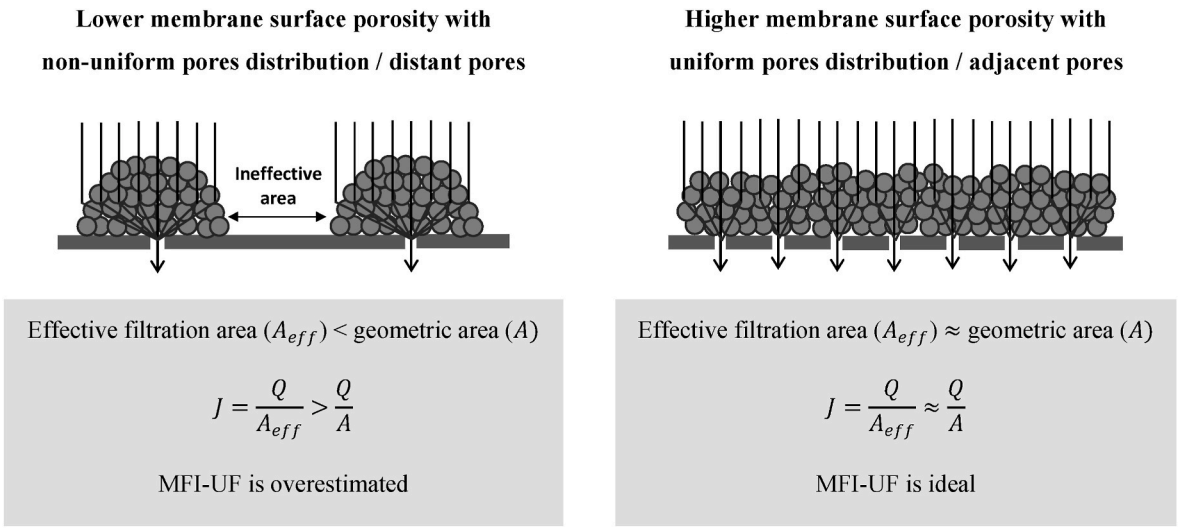

Fig. 14. Schematic diagram illustrating the structure of the polystyrene particles cake formed on membrane with low and high surface porosity and uniform and non-uniform pore distribution.

Table 2
MFI-UF preliminary correction factors for the effect of membrane surface porosity (based on washed polystyrene particles suspension).

Membrane MWCO	5 kDa	10 kDa	50 kDa	100 kDa
MFI-UF correction factor	0.4	0.5	0.6	1.0

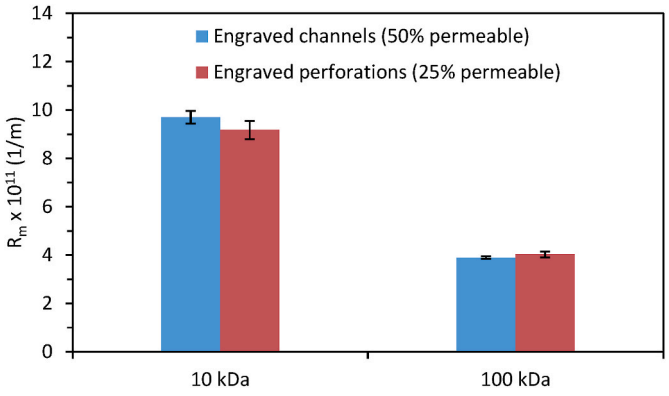

Fig. 15. R_m of 10 and 100 kDa membranes measured based on both sides of the holder support pad.

structure of the MF and UF membranes. The cross-section of the 0.45 MF membrane consists of only one layer where the pores extend from the top to the bottom of the membrane [43]. Therefore, in the study of Nahrstedt and Camargo-Schmale [29] and Salinas Rodriguez et al. [30], the pores of the MF membrane were in direct contact with the support pad. As a result, the non-permeable part of the pad blocked the pores which were in contact with it, and consequently reduced the surface porosity of the MF membrane. On the other hand, the cross-section of the UF membranes used in this work has a composite structure consisting of two main parts; a filtration layer with interconnected pores in the top, and a supporting base layer in the bottom [16]. Therefore, the top filtration layer of UF membrane (i.e. membrane pores) was not affected by the pad as there was no direct contact with it, as the lower layer of membrane (bottom layer) was in between. In addition, the interconnectivity of the pores of UF membranes could also allow the water to flow through the membrane via different routes even if the pad blocked some of membrane pores.

4.5. *Effect of membrane surface porosity on the prediction of particulate fouling in a full-scale RO plant*

Table 3 and Fig. 16 show the inputs and the outputs of the MFI-UF fouling prediction model (Equation (7)), respectively. The MFI-UF values were calculated both before and after correcting for the effect of non-uniform membrane surface porosity. No further correction for the membrane holder support pad was incorporated since no impact was found on the MFI-UF due to the support pad.

4.5.1. *Actual fouling observed in the RO plant*

Fig. 16 shows also the NDP increase observed in an RO plant in the period after MFI-UF measurements. It should be noted that the observed NDP increase in the RO plant can be due to a number of fouling phenomena such as scaling, biological fouling, organic fouling and/or particulate/colloidal fouling or a combination of all of the above. Although, the various types cannot be ruled out completely, fouling in this plant was attributed mainly to particulates/colloids (i.e. formation of cake/gel by particles/colloids accumulated on the RO membrane surface) for the following reasons.

Firstly, even though the concentrate in first stage (R = 57%) is supersaturated with respect to calcium carbonate (saturation index SI = 1) and barium sulphate (SI = 2.4), scaling is not expected to occur in the plant as antiscalant is dosed to the RO feed water (1.8 mg/L) to prevent precipitation of sparingly soluble salts. Moreover, the resulting saturation indices for both calcium carbonate and barium sulphate were low and in the range which can be easily controlled by the addition of antiscalant [44,45].

Secondly, the biofouling potential is also believed to be very low as the AOC concentration was well below 10 μg/L in the RO feed water during the prediction period (3–5 μg/L), which is often referred to as the

Table 3
Main inputs of the MFI-UF fouling prediction model (Equation (7)).

Membrane MWCO	10 kDa	5 kDa
MFI-UF of RO feed (without | with correction)	1580 s/L^2 | 790 s/L^2	2130 s/L^2 | 850 s/L^2
MFI-UF of RO conc. (without | with correction)	2440 s/L^2 | 1220 s/L^2	3200 s/L^2 | 1280 s/L^2
Deposition factor (Ω)	0.59	0.62
Flux (J)	26 L/m^2.h	
Viscosity (at normalized temperature of 25 °C)	0.00089 N s/m^2	

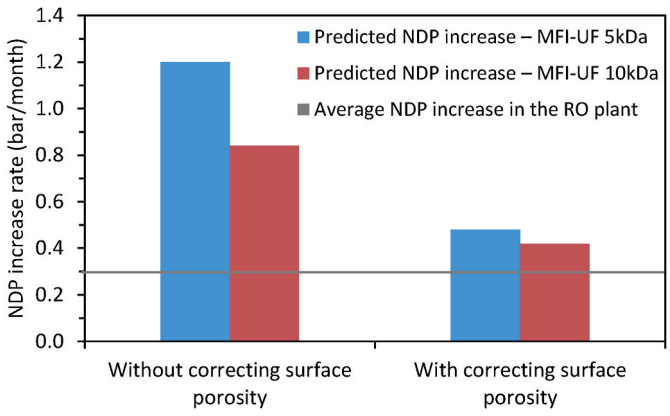

Fig. 16. Predicted NDP increase rates with and without correcting the MFI-UF for the effect of non-uniform membrane surface porosity.

threshold level to avoid biological fouling [46–49]. Moreover, the TEP concentration in the RO feed water, which may help to kick-start biological fouling, was also very low (0.26 mgXeq/L) [50].

Thirdly, organic fouling (DOC concentration <2.6 mg/L) due to the adsorption of organic matter directly onto the surface of the RO membrane is expected to occur prior to cake/gel formation when new/clean membranes are put into operation. However, in this case the RO membranes were already in operation for around 6 months (with membrane cleaning in place (CIP) performed only 2 times per year). Hence, the contribution of organic fouling is believed to be low and limited to the period of operation prior to cake/gel formation on the membrane.

Based on the above, the most likely type of fouling to occur in the RO plant is particulate/colloidal fouling as reflected by the MFI-UF measured for the RO feed water. The presence of particulate/colloidal matter in the RO feed (particularly after UF pre-treatment) may be due to (i) the passage of small colloids through the UF (150 kDa) which could be captured by the MFI-UF membrane (5–10 kDa) (ii) loss of integrity of the UF (i.e. broken fibres), which could allow particles/colloids to pass into the permeate stream (the UF integrity test is performed regularly in the plant, but loss in integrity might have occurred during the prediction period), (iii) re-aggregation of small particles/colloids that passed through the UF in the buffer tank located after the UF and prior to the RO, and/or (iv) re-growth of bacteria on the permeate side of the UF membrane (which are considered as particles).

4.5.2. Comparing actual and predicted particulate fouling rates in an RO plant

The NDP increase predicted based on the MFI-UF measured with 10 and 5 kDa membranes were substantially overestimated before correcting the effect of membrane surface porosity, i.e. the predicted rates of increase in NDP were about 3.0–4.5 times higher than the actual rate of increase in NDP observed in the RO plant (0.27 bar/month). However, after correcting the effect of membrane surface porosity, the difference between the predicted and observed NDP decreased to 1.6–1.8 times, improving the prediction by around 50–60%.

Despite the improvement obtained by correcting the effect of membrane surface porosity, the NDP increase predicted based on the 10 and 5 kDa membranes was still overestimated. The reason is most likely due to the fact that the correction factors were obtained based on a feed suspension of (synthetic) monodisperse polystyrene particles, which are rigid and thus hardly compressible. On the other hand, natural water (i.e. RO feed) comprises many different types of particles which are likely to be more deformable and compressible (such as the particulate/colloidal organic material released by bacteria and algae). In addition, particles in natural water are expected to have a wider range of sizes, shapes and densities. Subsequently, small particles can fill the voids between the larger particles in the cake formed on the MFI-UF membranes. Hence, the cake formed by natural particles might be more compressed and less porous than that formed by (rigid) polystyrene particles. Consequently, since the MFI-UF is highly dependent on cake porosity (Equation (6)), the effect of non-uniform distribution of membrane pores on the cake and thus on the MFI-UF might be greater for real RO feed/concentrate than for a polystyrene particle suspension. As a result, the preliminary correction factors estimated based on (synthetic) polystyrene particles might have underestimated the effect of non-uniform membrane surface porosity on the MFI-UF of real RO feedwater.

Therefore, future research (using the approach developed in this work) to understand the effect of non-uniform membrane surface porosity should focus on searching for and testing different types of particles (and mixtures of particles) which exhibit similar properties to natural particles existing in real water (i.e. RO feed)

5. Conclusions and recommendations

This study investigated the effect of surface porosity on the MFI-UF, measured at constant flux, with flat-sheet PES UF membranes with a MWCO of 5, 10, 50 and 100 kDa. The following were the main conclusions:

- Ultra-high resolution SEM analysis showed that the lower the membrane MWCO, the lower the membrane surface porosity, and the more non-uniformly the pores are distributed over membrane surfaces.
- A new approach, using suspensions of pre-washed polystyrene particles (75 nm), was successfully developed and applied to experimentally verify and quantify the effect of membrane surface porosity on the MFI-UF independently of membrane pore size.
- Based on the results of the newly developed approach, the MFI-UF was found to be highly dependent on membrane surface porosity; i.e. pore distribution over the membrane surface. The results indicated that in case of a non-uniform distribution of pores, cake formation might not be distributed evenly over the entire membrane surface and may be limited only to the porous regions. This results in a smaller effective filtration area, and subsequently a higher local flux, which eventually leads to overestimation of the measured MFI-UF.
- Accordingly, preliminary correction factors of 0.4, 0.5, 0.6 and 1.0 were identified to correct the MFI-UF for the effect of surface porosity of the 5, 10, 50 and 100 kDa membrane, respectively.
- Correcting the MFI-UF for the effect of membrane surface porosity significantly improved the prediction of particulate fouling in a full-scale RO plant, by around 50–60%. Nevertheless, despite the improvement, the predicted particulate fouling rate was still overestimated. The reason was attributed to the difference in the properties of polystyrene particles (used to estimate the correction factors) and natural particles which exist in real RO feedwater (the cake formed by natural particles may have lower porosity and thus higher resistance compared to that formed by rigid synthetic polystyrene particles).

In addition, the findings of this study can be used as a basis for recommended investigations for future research, including:

- Investigating and quantifying the effect of membrane surface porosity using different types of organic and inorganic particles (and mixtures of particles) which exhibit similar properties to particles that exist in real water (e.g. RO feed). Eventually, 'global' correction factors should be proposed for different types of feed water.
- Investigating the effect of membrane surface porosity for higher MWCO UF membranes (i.e. with higher surface porosity); verifying the assumption that there is low/negligible effect due to surface porosity on the MFI-UF with membranes of MWCO ≥100 kDa. However, the size of tested particles should be further investigated in

this case (as membrane pore size is expected to be higher with MWCO ≥100 kDa) to ensure the criterion of complete particle retention (i.e. to quantify the effect of membrane surface porosity independently of membrane pore size).
- In addition to the effect of membrane surface porosity investigated in this study, further work is required to examine also the effect of pore size distribution on the measured MFI-UF and thus on the predicted particulate fouling rate. This can give a more complete picture of the overall effect of membrane surface properties on particulate fouling prediction.

Author statement

Mohanad Abunada: Conceptualization, Methodology, Validation, Formal analysis, Investigation, Writing - Original Draft, Visualization, Project administration. **Nirajan Dhakal:** Conceptualization, Methodology, Writing - Review & Editing, Supervision. **William Z. Andyar:** Investigation. **Pamela Ajok:** Investigation. **Herman Smit:** Resources. **Noreddine Ghaffour:** Resources. **Jan C. Schippers:** Conceptualization, Methodology, Writing - Review & Editing. **Maria D. Kennedy:** Conceptualization, Methodology, Writing - Review & Editing, Supervision.

Declaration of competing interest

The authors declare that they have no known competing financial interests or personal relationships that could have appeared to influence the work reported in this paper.

Data availability

No data was used for the research described in the article.

Acknowledgements

This study has received funding from the European Union's Horizon 2020 research and innovation programme under grant agreement No. 820906 and the Department of Biotechnology (Government of India, Project No. BT/IN/EU-WR/40/AM/2018). The authors would like to acknowledge Alla Alpatova from King Abdullah University of Science and Technology (KAUST) for her contribution in imaging the UF membrane surfaces by SEM. Thanks also to Alma Imamovic from IHE-Delft Institute for Water Education (IT department) for her help in taking the pictures of the membrane holder support pad.

Appendix A. Supplementary data

Supplementary data to this article can be found online at https://doi.org/10.1016/j.memsci.2022.120854.

References

[1] A. Alpatova, A. Qamar, M. Al-Ghamdi, J. Lee, N. Ghaffour, Effective membrane backwash with carbon dioxide under severe fouling and operation conditions, J. Membr. Sci. 611 (2020), 118290, https://doi.org/10.1016/j.memsci.2020.118290.
[2] ASTM, ASTM D4189-07, Standard Test Method for Silt Density Index (SDI) of Water, West Conshohocken, PA, USA, 2014.
[3] ASTM, ASTM D8002-15, Standard Test Method for Modified Fouling Index (MFI-0.45) of Water, West Conshohocken, PA, USA, 2015.
[4] A. Alhadidi, B. Blankert, A.J.B. Kemperman, J.C. Schippers, M. Wessling, W.G. J. van der Meer, Effect of testing conditions and filtration mechanisms on SDI, J. Membr. Sci. 381 (1–2) (2011) 142–151, https://doi.org/10.1016/j.memsci.2011.07.030.
[5] R.M. Rachman, N. Ghaffour, F. Wali, G.L. Amy, Assessment of silt density index (SDI) as fouling propensity parameter in reverse osmosis (RO) desalination systems, Desalination Water Treat. 51 (4–6) (2013) 1091–1103, https://doi.org/10.1080/19443994.2012.699448.
[6] A. Alhadidi, A.J.B. Kemperman, B. Blankert, J.C. Schippers, M. Wessling, W.G. J. van der Meer, Silt Density Index and Modified Fouling Index relation, and effect of pressure, temperature and membrane resistance, Desalination 273 (1) (2011) 48–56, https://doi.org/10.1016/j.desal.2010.11.031.
[7] A. Alhadidi, A.J.B. Kemperman, J.C. Schippers, B. Blankert, M. Wessling, W.G. J. van der Meer, SDI normalization and alternatives, Desalination 279 (1–3) (2011) 390–403, https://doi.org/10.1016/j.desal.2011.06.042.
[8] J.C. Schippers, J. Verdouw, The modified fouling index, a method of determining the fouling characteristics of water, Desalination 32 (1980) 137–148, https://doi.org/10.1016/S0011-9164(00)86014-2.
[9] J.C. Schippers, H.C. Folmer, J. Verdouw, H.J. Scheerman, Reverse osmosis for treatment of surface water, Desalination 56 (1985) 109–119, https://doi.org/10.1016/0011-9164(85)85018-9.
[10] S.F.E. Boerlage, M. Kennedy, M.P. Aniye, J.C. Schippers, Applications of the MFI-UF to measure and predict particulate fouling in RO systems, J. Membr. Sci. 220 (1–2) (2003) 97–116, https://doi.org/10.1016/S0376-7388(03)00222-9.
[11] S.F.E. Boerlage, M.D. Kennedy, M.P. Aniye, E. Abogrean, Z.S. Tarawneh, J. C. Schippers, The MFI-UF as a water quality test and monitor, J. Membr. Sci. 211 (2) (2003) 271–289, https://doi.org/10.1016/S0376-7388(02)00427-1.
[12] S.F.E. Boerlage, M.D. Kennedy, M.p. Aniye, E.M. Abogrean, D.E.Y. El-Hodali, Z. S. Tarawneh, J.C. Schippers, Modified fouling index ultrafiltration to compare pretreatment processes of reverse osmosis feedwater, Desalination 131 (1) (2000) 201–214, https://doi.org/10.1016/S0011-9164(00)90019-5.
[13] S.F.E. Boerlage, M.D. Kennedy, M.P. Aniye, E.M. Abogrean, G. Galjaard, J. C. Schippers, Monitoring particulate fouling in membrane systems, Desalination 118 (1) (1998) 131–142, https://doi.org/10.1016/S0011-9164(98)00107-6.
[14] S.F.E. Boerlage, M.D. Kennedy, P.A.C. Bonne, G. Galjaard, J.C. Schippers, Prediction of flux decline in membrane systems due to particulate fouling, Desalination 113 (2) (1997) 231–233, https://doi.org/10.1016/S0011-9164(97)00134-3.
[15] S.F.E. Boerlage, M. Kennedy, Z. Tarawneh, R. De Faber, J.C. Schippers, Development of the MFI-UF in constant flux filtration, Desalination 161 (2) (2004) 103–113, https://doi.org/10.1016/S0011-9164(04)90046-X.
[16] S.G. Salinas-Rodríguez, G.L. Amy, J.C. Schippers, M.D. Kennedy, The modified fouling index ultrafiltration constant flux for assessing particulate/colloidal fouling of RO systems, Desalination 365 (2015) 79–91, https://doi.org/10.1016/j.desal.2015.02.018.
[17] Y. Jin, Y. Ju, H. Lee, S. Hong, Fouling potential evaluation by cake fouling index: theoretical development, measurements, and its implications for fouling mechanisms, J. Membr. Sci. 490 (2015) 57–64, https://doi.org/10.1016/j.memsci.2015.04.049.
[18] J.-S. Choi, T.-M. Hwang, S. Lee, S. Hong, A systematic approach to determine the fouling index for a RO/NF membrane process, Desalination 238 (1) (2009) 117–127, https://doi.org/10.1016/j.desal.2008.01.042.
[19] Y. Yu, S. Lee, K. Hong, S. Hong, Evaluation of membrane fouling potential by multiple membrane array system (MMAS): measurements and applications, J. Membr. Sci. 362 (1–2) (2010) 279–288, https://doi.org/10.1016/j.memsci.2010.06.038.
[20] Y. Ju, I. Hong, S. Hong, Multiple MFI measurements for the evaluation of organic fouling in SWRO desalination, Desalination 365 (2015) 136–143, https://doi.org/10.1016/j.desal.2015.02.035.
[21] L.N. Sim, Y. Ye, V. Chen, A.G. Fane, Crossflow sampler modified fouling index ultrafiltration (CFS-MFIUF)—an alternative fouling index, J. Membr. Sci. 360 (1–2) (2010) 174–184, https://doi.org/10.1016/j.memsci.2010.05.010.
[22] L.N. Sim, Y. Ye, V. Chen, A.G. Fane, Comparison of MFI-UF constant pressure, MFI-UF constant flux and crossflow sampler-modified fouling index ultrafiltration (CFS-mfiuf), Water Res. 45 (4) (2011) 1639–1650, https://doi.org/10.1016/j.watres.2010.12.001.
[23] A.G. Fane, C.J.D. Fell, P.H. Hodgson, G. Leslie, K.C. Marshall, Microfiltration of biomass and biofluids: effects of membrane morphology and operating conditions, Filtrat. Separ. 28 (5) (1991), https://doi.org/10.1016/0015-1882(91)80157-Z, 332-331.
[24] S.F.E. Boerlage, M.D. Kennedy, M.R. Dickson, D.E.Y. El-Hodali, J.C. Schippers, The modified fouling index using ultrafiltration membranes (MFI-UF): characterisation, filtration mechanisms and proposed reference membrane, J. Membr. Sci. 197 (1–2) (2002) 1–21, https://doi.org/10.1016/S0376-7388(01)00618-4.
[25] S.G. Salinas-Rodriguez, Particulate and Organic Matter Fouling of Seawater Reverse Osmosis Systems: Characterization, Modelling and Applications, first ed., CRC Press/Balkema, London, UK, 2011.
[26] C. Güell, R.H. Davis, Membrane fouling during microfiltration of protein mixtures, J. Membr. Sci. 119 (2) (1996) 269–284, https://doi.org/10.1016/0376-7388(96)80001-J.
[27] M. Chandler, A. Zydney, Effects of membrane pore geometry on fouling behavior during yeast cell microfiltration, J. Membr. Sci. 285 (1) (2006) 334–342, https://doi.org/10.1016/j.memsci.2006.09.002.
[28] C.R. Ethier, R.D. Kamm, The hydrodynamic resistance of filter cakes, J. Membr. Sci. 43 (1) (1989) 19–30, https://doi.org/10.1016/S0376-7388(00)82350-9.
[29] A. Nahrstedt, J. Camargo-Schmale, New insights into silt density index and modified fouling index measurements, Water Sci. Technol. Water Supply 8 (4) (2008) 401–411, https://doi.org/10.2166/ws.2008.087.
[30] S.G. Salinas Rodriguez, N. Sithole, N. Dhakal, M. Olive, J.C. Schippers, M. D. Kennedy, Monitoring particulate fouling of North Sea water with SDI and new ASTM MFI0.45 test, Desalination 454 (2019) 10–19, https://doi.org/10.1016/j.desal.2018.12.006.
[31] P.C. Carman, Fundamental principles of industrial filtration (A critical review of present knowledge), Trans. Inst. Chem. Eng. 16 (1938) 168–188.

[32] J.C. Schippers, J.H. Hanemaayer, C.A. Smolders, A. Kostense, Predicting flux decline of reverse osmosis membranes, Desalination 38 (1981) 339–348, https://doi.org/10.1016/S0011-9164(00)86078-6.
[33] Y. Li, F. Gao, W. Wei, J.-B. Qu, G.-H. Ma, W.-Q. Zhou, Pore size of macroporous polystyrene microspheres affects lipase immobilization, J. Mol. Catal. B Enzym. 66 (1) (2010) 182–189, https://doi.org/10.1016/j.molcatb.2010.05.007.
[34] J.A. Brant, A.E. Childress, Assessing short-range membrane–colloid interactions using surface energetics, J. Membr. Sci. 203 (1–2) (2002) 257–273, https://doi.org/10.1016/S0376-7388(02)00014-5.
[35] K. Park, J.Y. Park, S. Lee, J. Cho, Measurement of size and number of suspended and dissolved nanoparticles in water for evaluation of colloidal fouling in RO membranes, Desalination 238 (1) (2009) 78–89, https://doi.org/10.1016/j.desal.2008.01.038.
[36] S.G. Yiantsios, A.J. Karabelas, The effect of colloid stability on membrane fouling, Desalination 118 (1) (1998) 143–152, https://doi.org/10.1016/S0011-9164(98)00110-6.
[37] P. Lipp, U. Müller, B. Hetzer, T. Wagner, Characterization of nanoparticulate fouling and breakthrough during low-pressure membrane filtration, Desalination Water Treat. 9 (1–3) (2009) 234–240, https://doi.org/10.5004/dwt.2009.812.
[38] D. Spettmann, S. Eppmann, H.-C. Flemming, J. Wingender, Simultaneous visualisation of biofouling, organic and inorganic particle fouling on separation membranes, Water Sci. Technol. 55 (8–9) (2007) 207–210, https://doi.org/10.2166/wst.2007.260.
[39] J. Lohaus, Y.M. Perez, M. Wessling, What are the microscopic events of colloidal membrane fouling? J. Membr. Sci. 553 (2018) 90–98, https://doi.org/10.1016/j.memsci.2018.02.023.
[40] T.A. Trinh, W. Li, J.W. Chew, Internal fouling during microfiltration with foulants of different surface charges, J. Membr. Sci. 602 (2020), 117983, https://doi.org/10.1016/j.memsci.2020.117983.
[41] D. Hund, S. Antonyuk, S. Ripperger, Simulation of bridging at the static surface filtration by CFD-DEM coupling, EPJ Web Conf. 140 (2017), 09033, https://doi.org/10.1051/epjconf/201714009033.
[42] R.S. Singh, G.K. Saini, J.F. Kennedy, Pullulan: microbial sources, production and applications, Carbohydr. Polym. 73 (4) (2008) 515–531, https://doi.org/10.1016/j.carbpol.2008.01.003.
[43] A. Alhadidi, A.J.B. Kemperman, J.C. Schippers, M. Wessling, W.G.J. van der Meer, The influence of membrane properties on the Silt Density Index, J. Membr. Sci. 384 (1–2) (2011) 205–218, https://doi.org/10.1016/j.memsci.2011.09.028.
[44] S.F.E. Boerlage, M.D. Kennedy, I. Bremere, G.J. Witkamp, J.P. Van der Hoek, J. C. Schippers, The scaling potential of barium sulphate in reverse osmosis systems, J. Membr. Sci. 197 (1) (2002) 251–268, https://doi.org/10.1016/S0376-7388(01)00654-8.
[45] M.N. Mangal, V.A. Yangali-Quintanilla, S.G. Salinas-Rodriguez, J. Dusseldorp, B. Blankert, A.J.B. Kemperman, J.C. Schippers, M.D. Kennedy, W.G.J. van der Meer, Application of a smart dosing pump algorithm in identifying real-time optimum dose of antiscalant in reverse osmosis systems, J. Membr. Sci. 658 (2022), https://doi.org/10.1016/j.memsci.2022.120717, 120717.
[46] M. Sousi, G. Liu, S.G. Salinas-Rodriguez, L. Chen, J. Dusseldorp, P. Wessels, J. C. Schippers, M.D. Kennedy, W. van der Meer, Multi-parametric assessment of biological stability of drinking water produced from groundwater: reverse osmosis vs. conventional treatment, Water Res. 186 (2020), 116317, https://doi.org/10.1016/j.watres.2020.116317.
[47] M. Sousi, S.G. Salinas-Rodriguez, G. Liu, J.C. Schippers, M.D. Kennedy, W. van der Meer, Measuring bacterial growth potential of ultra-low nutrient drinking water produced by reverse osmosis: effect of sample pre-treatment and bacterial inoculum, Front. Microbiol. 11 (2020), https://doi.org/10.3389/fmicb.2020.00791.
[48] P.W.J.J. van der Wielen, D. van der Kooij, Effect of water composition, distance and season on the adenosine triphosphate concentration in unchlorinated drinking water in The Netherlands, Water Res. 44 (17) (2010) 4860–4867, https://doi.org/10.1016/j.watres.2010.07.016.
[49] A. Abushaban, S.G. Salinas-Rodriguez, N. Dhakal, J.C. Schippers, M.D. Kennedy, Assessing pretreatment and seawater reverse osmosis performance using an ATP-based bacterial growth potential method, Desalination 467 (2019) 210–218, https://doi.org/10.1016/j.desal.2019.06.001.
[50] L.O. Villacorte, Y. Ekowati, H.N. Calix-Ponce, J.C. Schippers, G.L. Amy, M. D. Kennedy, Improved method for measuring transparent exopolymer particles (TEP) and their precursors in fresh and saline water, Water Res. 70 (2015) 300–312, https://doi.org/10.1016/j.watres.2014.12.012.